Molecular Biology of the Cell
Vol. 16, 5793–5803, December 2005

Dynamic Partitioning into Lipid Rafts Controls the Endo-Exocytic Cycle of the $\alpha L/\beta_2$ Integrin, LFA-1, during Leukocyte Chemotaxis[D]

Monica Fabbri,*† Silvia Di Meglio,*† Maria Cristina Gagliani,‡ Elisa Consonni,* Raffaella Molteni,* Jeffrey R. Bender,§ Carlo Tacchetti,‡ and Ruggero Pardi*

*Unit of Leukocyte Biology, Vita-Salute San Raffaele University School of Medicine, DIBIT-Scientific Institute San Raffaele, 20132 Milan, Italy; ‡MicroSCoBiO Research Center and IFOM Center of Cell Oncology and Ultrastructure, Department of Experimental Medicine, University of Genova, 16132 Genoa, Italy; and §Raymond and Beverly Sackler Foundation Cardiovascular Laboratory, Sections of Cardiovascular Medicine and Immunobiology, Yale University School of Medicine, New Haven, CT 06536

Submitted May 10, 2005; Revised September 20, 2005; Accepted September 23, 2005
Monitoring Editor: Martin A. Schwartz

Cell migration entails the dynamic redistribution of adhesion receptors from the cell rear toward the cell front, where they form new protrusions and adhesions. This process may involve regulated endo-exocytosis of integrins. Here we show that in primary neutrophils unengaged $\alpha L/\beta_2$ integrin (LFA-1) is internalized and rapidly recycled upon chemoattractant stimulation via a clathrin-independent, cholesterol-sensitive pathway involving dynamic partitioning into detergent-resistant membranes (DRM). Persistent DRM association is required for recycling of the internalized receptor because 1) >90% of endocytosed LFA-1 is associated with DRM, and a large fraction of the internalized receptor colocalizes intracellularly with markers of DRM and the recycling endocytic compartment; 2) a recycling-defective mutant ($\alpha L/\beta_2^{Y735A}$) dissociates rapidly from DRM upon being endocytosed and is subsequently diverted into a late endosomal pathway; and 3) a dominant negative Rab11 mutant ($Rab11^{S25N}$) induces intracellular accumulation of endocytosed $\alpha L/\beta_2$ and prevents its enrichment in chemoattractant-induced lamellipodia. Notably, chemokine-induced migration of neutrophils over immobilized ICAM-1 is abrogated by cholesterol-sequestering agents. We propose that DRM-associated endocytosis allows efficient retrieval of integrins, as they detach from their ligands, followed by polarized recycling to areas of the plasma membrane, such as lamellipodia, where they establish new adhesive interactions and promote outside-in signaling events.

INTRODUCTION

Cell migration is a highly dynamic process featuring a defined sequence of tightly regulated steps. These include extension of a membrane protrusion, formation of stable attachments near the leading edge of the protrusion, translocation of the cell body forward, release of adhesions, and retraction at the cell rear (Ridley *et al*., 2003). Directional migration involves the establishment and maintenance of a spatial and functional asymmetry of adhesion- and migration-related molecular components between the anterior (leading) and posterior (trailing) edges of the migrating cell (Lauffenburger and Horwitz, 1996; Ridley *et al*., 2003). Such asymmetric distribution, or polarization, is largely conserved between amoebae and mammalian cells (Manahan *et al*., 2004). Spatial asymmetry involves the dynamic redistribution of adhesion and chemotactic receptors, signaling molecules, and cytoskeletal components along the anterior-posterior axis of the chemotaxing cell (Manes *et al*., 2003). The mechanistic role played by spatial asymmetry of signaling networks in directional motility is exemplified by the unequal distribution of the lipid phosphatase with sequence homology to tensin (PTEN) in chemotaxing cells (Devreotes and Janetopoulos, 2003; Merlot and Firtel, 2003). By being recruited to the posterior edge of migrating cells, PTEN contributes to establishing an internal anterior-posterior gradient of the phosphatidylinositol 3,4,5-phosphate lipid messenger, which is required to impart directionality to the moving cell (Funamoto *et al*., 2002; Iijima and Devreotes, 2002). Likewise, the Ca^{2+}-dependent protease calpain has been proposed to differentially regulate integrin-containing complexes at the rear and front edges of migrating cells (Lokuta *et al*., 2003). Selected lipid constituents of the plasma membrane also relocalize asymmetrically in migrating cells, with lipid rafts, consisting of liquid-ordered microdomains enriched in glycosphingolipids and cholesterol, becoming coalescent and microscopically visible at both edges (Simons and Ikonen, 1997; Manes *et al*., 1999). How such coordinate

This article was published online ahead of print in *MBC in Press* (http://www.molbiolcell.org/cgi/doi/10.1091/mbc.E05–05–0413) on October 5, 2005.

[D] The online version of this article contains supplemental material at *MBC Online* (http://www.molbiolcell.org).

† These authors contributed equally to this work.

Address correspondence to: Monica Fabbri (fabbri.monica@hsr.it).

Abbreviations used: cav-1, caveolin1; DRM, detergent-resistant membrane(s); fpR, *N*-formyl peptide receptor; GFP, green fluorescent protein; HAfpR-CHO, Chinese hamster ovary cells stably transfected with hemagglutinin-*N*-formyl peptide receptor; PMN, polymorphonuclear cell(s); TfR, transferrin receptor; WGA, wheat germ agglutinin.

redistribution of molecular components of the cell migration and signaling machinery is controlled and maintained over time is largely unknown. Particularly relevant is the issue of membrane raft microdomain relocalization in chemotaxing leukocytes (Gomez-Mouton *et al*., 2001; Millan *et al*., 2002). Lipid rafts have been proposed to act as signaling platforms by recruiting distinct sets of signaling pathways whose core components display high affinity for the liquid-ordered environment of rafts (Simons and Toomre, 2000). The appearance of asymmetrically distributed raft microdomains in chemotactically stimulated cells could affect the polarized recruitment and local activation of raft-associated proteins and lipid messengers, such as phosphatidyl inositol phosphates, which are required for chemoattractant sensing and directional migration (McKay *et al*., 1991; Manes *et al*., 2003). The current dogma states that clustering of raft resident proteins, such as glycosyl phosphatidyl inositol (GPI)-anchored molecules, or raft-associated cytoskeletal components is required to dynamically control the local density of submicroscopic raft microdomains (Varma and Mayor, 1998; Fivaz *et al*., 2002). However, polarized cells display raft-enriched membrane microdomains, well above the threshold of microscopic detection, in defined areas of the plasmalemma and in the apparent absence of raft clustering (Manes *et al*., 2003). This has been shown to occur at the apical side of polarized epithelial cells as well as at the leading edge of migrating leukocytes (Eaton and Simons, 1995; Manes *et al*., 2000). Thus, alternative mechanisms must exist to establish and maintain the asymmetric distribution of raft microdomains. Two non-mutually exclusive mechanisms could account for the emergence of asymmetrically distributed lipid rafts in migrating cells: raft-resident proteins and lipids could diffuse laterally in a stimulus-dependent manner to become enriched in defined areas of the plasmalemma. Alternatively, raft constituents could be subject to a polarized exo-endocytic cycle leading to the progressive enrichment of selected lipid raft constituents in defined areas of the plasma membrane of chemotaxing cells (Eaton and Simons, 1995; Bretscher and Aguado-Velasco, 1998). We sought to investigate this issue by following the distribution of both endogenous and ectopically expressed leukocyte integrins in cells exposed to a chemotactic stimulus, because integrins have been shown to be dynamically recruited into lipid rafts upon cell stimulation (Krauss and Altevogt, 1999; Leitinger and Hogg, 2002). Leukocyte-specific integrins promote migration by interacting with cell surface-expressed ligands during the extravasation process (Springer, 1994; Bianchi *et al*., 1997; Fabbri *et al*., 1999a). Several studies have shown that integrin-containing vesicles move from the rear of the cell to a perinuclear region (Lawson and Maxfield, 1995). Additional evidence shows that integrin-containing vesicles move from the perinuclear region to the base of the lamellipodium in fibroblasts, and to an endosomal recycling compartment near the cell front in neutrophils (Pierini *et al*., 2000, 2003).

The endocytic cycle of integrins in vectorially migrating cells is poorly characterized at the molecular level. It is also not known whether recycling of endocytosed adhesion molecules from the rear and/or the leading edge represents a significant mechanism for supplying materials to the cell front. Among the unsolved issues is the nature of the endocytic vesicles stemming from areas of the plasma membrane enriched in integrins, and whether such early steps occur in specialized areas of the plasma membrane. Here, we investigated in detail the endocytic pathway followed by unengaged leukocyte integrins in primary neutrophils as well as in fibroblastoid cells. We show that the integrin's endo-exocytic cycle requires dynamic, chemokine-regulated partitioning into lipid rafts and that endocytosed, recycling-competent integrins display a persistent association with DRM, which is required for their polarized recycling to the emerging lamellipodia. We propose that the above-mentioned process may contribute to the generation of membrane protein and lipid asymmetry in directionally migrating cells.

MATERIALS AND METHODS

Antibodies and Reagents

Monoclonal antibody (mAb) TS1.22 (anti-αL) was kindly provided by T. A. Springer (Harvard Medical School, Boston, MA). mAbs anti-αL clone 27, anti-flotillin-2 clone 29, anti-LAMP-1, and anti-Rab11 clone 47 were from BD Biosciences (San Jose, CA). mAb anti-rat β_2 clone WT3 was purchased from American Type Culture Collection (Manassas, VA). Anti-CD4 mAb clone S3.5 was a kind gift of E. Engleman (Stanford University, Stanford, CA). Anti-EEA-1 mAb was from Santa Cruz Biotechnology (Santa Cruz, CA). Horseradish peroxidase (HRP)-conjugated goat anti-mouse and rabbit anti-Rab11 antisera were purchased from Zymed Laboratories (South Francisco, CA). Anti-transferrin receptor (TfR) antibodies included mAb clone 5E9C11 (American Type Culture Collection) and mAb clone B3/25 (Roche Diagnostics, Indianapolis, IN). β-Methylcyclodextrin, filipin, tetramethylrhodamine B isothiocyanate (TRITC)-conjugated wheat germ agglutinin (WGA), *N*-formyl-L-methionyl-L-leucyl-L-phenylalanine (fMLF), glutathione, and anti-HRP mAb were from Sigma-Aldrich (Milan, Italy). Ez-Link NHS-SS-biotin was from Pierce Chemical (Rockford, IL). Recombinant zz-intercellular adhesion molecule (ICAM)-1 was a kind gift of R. Solari (GlaxoSmithKline, Uxbridge, Middlesex, United Kingdom). The anti-αL Fab' fragment was obtained by immobilized papain digestion of mAb TS1.22 followed by purification by gel filtration.

DNA Constructs

The cDNAs containing the coding region of the αL and β_2 subunits subcloned into the expression vector pCDM8 were kindly provided by T. A. Springer (Harvard University, Boston, MA). The αL-green fluorescent protein (GFP) and the β_2^{Y735A} cDNA were cloned as described previously (Fabbri *et al*., 1999a). The Rab11^{S25N} mutant, cloned into the pGEM I vector, was a kind gift of J. Salamero (Institute Curie, Paris, France): the cDNA was cloned into the expression vector pcDNAI (Invitrogen, Carlsbad, CA) by the unique restriction sites *Bam*HI and *Pst*I. The construct coding for Rab11^{S25N}-GFP fusion protein was a kind gift of M. Zerial (Dresden, Germany). The constructs coding for mDSred-tagged rab11 wild type (wt) and the S25N mutant were obtained by PCR amplification with primers that introduced the unique cloning sites Xho and BamHI, followed by digestion and cloning into pDSRed-monomer-C1 (BD Biosciences, Palo Alto, CA). The cDNA containing the coding region of *N*-formyl peptide receptor (fpR) tagged to the hemagglutinin (HA) epitope was a kind gift of Silvano Sozzani (University of Brescia, Brescia, Italy). The cDNA coding for the human transferrin receptor, Eps15 wt, and Δ95-295 mutant were a kind gift of P. Di Fiore (IFOM, Milan, Italy); the cDNA coding for Rab5 wt and N133I mutant were kind gifts of C. Bucci (University of Lecce, Lecce, Italy); and the cDNA coding for dynamin wt and K44A mutant were a kind gift of S. Schmid (The Scripps Research Institute, La Jolla, CA).

Cell Culture

Polymorphonuclear cells (PMN) were isolated from fresh heparinized blood of healthy human volunteers by dextran sedimentation, followed by Ficoll-Hypaque gradient centrifugation as described previously (Clark and Nauseef, 1996). Contaminating red cells were removed by NH_4Cl lysis. Chinese hamster ovary (CHO) cells were maintained in α-minimal essential medium (Invitrogen, S. Giuliano Milanese, Milan, Italy) with 10% fetal calf serum (Hyclone Laboratories, Logan, UT). For HA-fpR stable transfectants, CHO cells were transfected with the HA-fpR cDNA with LipofectAMINE. After 72 h, selection with 1 mg/ml G418 (Roche Diagnostics) was started. Surviving cells were subcloned, expanded, and tested for HA-fpR surface expression by flow cytometry.

Floatation Assays

Sucrose gradient analysis was performed according to previously published protocols (Brown and Rose, 1992; Zurzolo *et al*., 1994). Either CHO cells (2 × 150-mm dishes grown to 80% confluence) or PMN (20×10^6) were rinsed in phosphate-buffered saline (PBS) and lysed in 25 mM 2-(*N*-morpholino)ethanesulfonic acid, 150 mM NaCl, and 1% Triton X-100 (MBS buffer) on ice. Lysates were brought to 40% sucrose and placed at the bottom of a centrifuge tube. A step sucrose gradient (5–35% in MBS buffer) was layered on top of the lysates, and the samples were centrifuged at 39,000 rpm for 18–20 h in a

Beckman SW41 rotor (Beckman Coulter, Fullerton, CA). One-milliliter fractions were harvested from the top of the gradient. Collected fractions were trichloroacetic acid precipitated and run on SDS-PAGE. After transfer to nitrocellulose, proteins were detected by hybridization with specific antibodies and revealed by the enhanced chemiluminescence (ECL) detection system (GE Healthcare, Little Chalfont, Buckinghamshire, United Kingdom).

Internalization and Recycling Assay

Internalization and recycling were evaluated as described previously (Fabbri *et al*., 1999a). Briefly, for the internalization assay, plastic-adherent CHO transfectants or suspended PMN (5×10^6) were washed in PBS and incubated in the absence or presence of 5 μg/ml filipin at 37°C for 45 min. Cells were then incubated 1 h on ice in presence of 0.5 mg/ml NHS-SS-biotin in PBS. Labeled cells were incubated for the indicated times at 37°C in serum-free medium to allow internalization. Samples were then returned to ice, washed, and treated with two successive reductions of 20 min with a reducing solution containing 42 mM glutathione, 75 mM NaCl, 1 mM EDTA, 1% bovine serum albumin, and 75 mM NaOH. Cells were then washed, collected by scraping, and lysed in 500 μl of a solution containing 10 mM Tris, 150 mM NaCl, 1 mM $CaCl_2$, 1 mM $MgCl_2$, and 1% NP-40 on ice. $\alpha L/\beta_2$ was immunoprecipitated from lysates (anti-αL TS1.22) and eluted in nonreducing sample buffer. Samples were analyzed by SDS-PAGE, transferred onto nitrocellulose, and revealed with HRP-conjugated avidin (GE Healthcare), stripped in the presence of reducing agents, and incubated with anti-αL mAb clone 27 followed by HRP-conjugated goat anti-mouse, for normalization. The peroxidase reaction was developed using ECL (GE Healthcare). For the analysis of recycling, internalization was allowed for 5 min (PMN) or 15 min (HAfpR-CHO) at 37°C. Samples were then reduced as described above. The internalized fraction was chased by incubation of duplicate samples at 37°C for the indicated time points. After the incubation, one of the two samples was reduced, to quantify the amount of protein that recycled back to the plasma membrane, whereas the other sample was not reduced, as a control. Samples were then collected and analyzed as described above. Recycling was calculated by subtracting the densitometric values of the residual biotinylated receptor, after incubation at 37°C and treatment with glutathione (GSH), from the total pool of internalized receptors. Band intensity was quantified by densitometry (GE Healthcare). In the experiments where the internalized fraction was subjected to flotation analysis, 3×150-mm dishes grown to 80% confluence of HAfpR-CHO were transfected with the indicated constructs. The internalization experiment was performed as described above, but cells were lysed in MBS buffer and subjected to a flotation assay. Floating and nonfloating fractions were pooled as described in *Results*, and $\alpha L/\beta_2$ was immunoprecipitated and revealed by Western blot with avidin-HRP before normalization with anti-αL mAb clone 27.

Immunofluorescence

For $\alpha L/\beta_2$ and Rab11 colocalization studies, HAfpR-CHO were transiently transfected with GFP-tagged $\alpha L/\beta_2$ and either mDSred-tagged rab11 wt or mDSred-tagged rab11^{S25N}. After 24 h, cells were fixed in 3.7% paraformaldehyde and inspected with a Spinning Disk Ultraview ERS (PerkinElmer, Wellesley, MA).

For colocalization of $\alpha L/\beta_2$ in PMN, 5×10^4 freshly purified PMN were incubated at 4°C with 100 μg/ml anti-αL (TS1.22) Fab′ fragment followed by incubation at 37°C for the indicated time points with 100 nM fMLF. Cells were then fixed in 3.7% paraformaldehyde, permeabilized with 0.1% Triton X-100, and stained with a Cy3-conjugated anti-mouse IgG antiserum. Rab11 staining was performed by incubation with rabbit anti-Rab11 antiserum, followed by a fluorescence isothiocyanate (FITC)-conjugated anti-IgG antiserum. LAMP-1 staining was performed by permeabilization in 0.4% saponin, incubation with mAb anti LAMP-1 (IgG_{2b}) followed by a FITC-conjugated anti-IgG_{2b} antiserum. Nuclei were labeled by Hoechst 33342 staining. Cells were then spun onto a slide by cytospin. For colocalization of $\alpha L/\beta_2$ in RBL, RBL cells were plated onto fibronectin-coated coverslips and treated at 4°C with 10 μg/ml anti-rat β_2 (WT3) followed by incubation at 37°C for the indicated time points with 100 nM fMLF. Cells were then fixed in 3.7% paraformaldehyde, permeabilized with 0.1% Triton X-100, and stained with a Cy3-conjugated anti-mouse IgG antiserum. Rab11 staining was performed by incubation with rabbit anti-Rab11 antiserum, followed by an FITC-conjugated anti-IgG antiserum. Nuclei were labeled by Hoechst 33342 staining. Cells were then inspected with a laser scanning confocal microscope (TCS SP2; Leica, Wetzlar, Germany).

For experiments assessing $\alpha L/\beta_2$ enrichment in rafts, HAfpR-CHO were transfected with αL-GFP/β_2. Twenty-four hours later, cells were starved without serum for 1 h followed by stimulation with 1 μM fMLF for 5′ at 37° and fixation in 3.7% paraformaldehyde. The plasma membrane was labeled with TRITC-conjugated WGA. Cells were then inspected with a laser scanning confocal microscope MRC-1024 (Bio-Rad, Hercules, CA), and the distribution analysis was performed as indicated in Table 1 legend.

For flow cytometry, HAfpR-CHO were transfected with $\alpha L/\beta_2$ and either Rab11^{S25N}-GFP or a mock construct. After 24 h, cells were starved without serum for 1 h followed by stimulation with 1 μM fMLF for 5′ at 37°. Cells were then transferred to ice, labeled with anti-αL mAb TS1.22 followed by Cy3-conjugated goat anti-mouse antibody and analyzed by flow cytometry using a FACScan cytometer equipped with a CellQuest software (BD Biosciences).

Migration Assay

Glass-bottom 35-mm dishes (MatTek, Ashland, MA) were coated with recombinant ICAM-1 as described previously (Fabbri *et al*., 1999b). Freshly purified PMN were resuspended at 0.5×10^6/ml in RPMI 1640 medium, treated in the presence or absence of 10 mM β-methylcyclodextrin or 5 μg/ml filipin for 45 min at 37°, plated onto coated dishes, and incubated at 37° for 30 min. Cells were then inspected by time-lapse microscopy at 37° for 20 min with a Zeiss Axiophot microscope equipped with a temperature-controlled stage. Analysis was performed using cell tracking software developed in-house, which uses gray scales to identify centroids in each cell inspected under a phase contrast microscope. Tracks of each single cell in time and space were recorded and movement quantified as the distance covered during the observation period. Because the chemokine was added in solution without a gradient, only the chemokinetic activity of cells, rather than their chemotaxis, could be quantified.

Electron Microscopy

Single and double immunogold localization on ultrathin cryosections were performed as described previously (Confalonieri *et al*., 2000). Briefly, 12% gelatin embedded, 2.3 M sucrose infused blocks of aldehyde-fixed $\alpha L/\beta 2$-CHO cells were frozen in liquid nitrogen. Ultrathin cryosections were obtained with a Reichert-Jung Ultracut E with FC4E cryoattachment and collected on copper-Formvar-carbon coated grids. Single and double immunogold localization on ultrathin cryosections were performed as described previously (Confalonieri *et al*., 2000). Labeling was revealed using 10- or 15-nm protein A-gold. All samples were examined with Philips CM10 or Fei Tecnai 12G2 electron microscopes.

RESULTS

$\alpha L/\beta_2$ Translocates into Lipid Rafts upon fpR Activation in Neutrophils

To investigate leukocyte integrin dynamics at the plasma membrane of chemokine-stimulated cells, we freshly purified PMN from human blood and analyzed the partitioning of $\alpha L/\beta_2$ in lipid rafts by flotation assays on 1% Triton X-100 lysates from unstimulated or fMLF-treated cells. As shown in Figure 1, a small but sizable fraction (1–2%) of $\alpha L/\beta_2$ is found in DRM in resting PMN. However, the amount of $\alpha L/\beta_2$ recovered in DRM increases (up to 18% depending on the donor) upon treatment of PMN with 100 nM fMLF for 5 min at 37° (Figure 1). Under these conditions, a fraction of the leukocyte integrin becomes associated with the detergent-insoluble pellet, possibly due to inducible connections with the actin-based cytoskeleton, which is largely insoluble in nonionic detergents (Figure 1A). As a control for flotation accuracy, we assessed the distribution of the raft resident protein flotillin-2 (Nebl *et al*., 2002; Slaughter *et al*., 2003) (Figure 1).

fMLF Stimulation Induces Cholesterol-dependent Endocytosis of Ligand-Free $\alpha L/\beta 2$

We next addressed whether chemokine stimulation affects the turnover of membrane-expressed $\alpha L/\beta_2$. In previous studies (Fabbri *et al*., 1999b; Tohyama *et al*., 2003), we had observed that ectopically expressed $\alpha L/\beta_2$ is constitutively internalized and recycled back to the plasma membrane at variable rates, depending on the cell type. In contrast, very little is known about the endocytic cycle of endogenous $\alpha L/\beta_2$ in primary leukocytes. To address this issue, we performed internalization and recycling assays in primary neutrophils in the absence or presence of 100 nM fMLF. Figure 2A shows that in unstimulated neutrophils $\alpha L/\beta_2$ seems to be relatively stable at the cell surface. On stimulation with fMLF, a considerable fraction (15–20%) of $\alpha L/\beta_2$ is rapidly endocytosed (Figure 2A, compare open circles with closed circles) in a ligand-independent manner. Interestingly, the internalized receptor is recycled rapidly to the cell

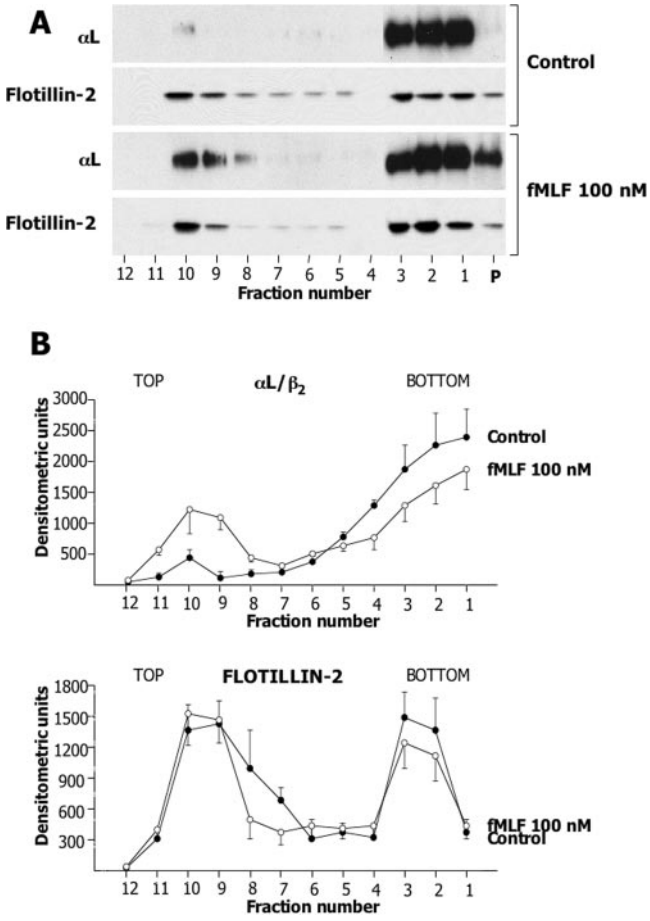

Figure 1. $\alpha L/\beta_2$ partitions into lipid rafts upon chemokine stimulation in PMN. (A) Freshly isolated PMN were incubated in the absence or presence of 100 nM fMLF for 5 min at 37°C, followed by lysis in 1% Triton X-100 and floatation on a discontinuous step sucrose gradient. The relative distribution of αL and the raft marker flotillin-2 were analyzed by Western blotting. (B) Densitometric analysis of a representative experiment showing the distribution of αL and flotillin-2 over a sucrose gradient in resting (control) or activated (100 nM fMLF) PMN.

surface, with >75% of the labeled pool being recycled after a 15-min chase (Figure 2B, open circles).

Because treatment of PMN with fMLF induces both partitioning of $\alpha L/\beta_2$ into lipid rafts and its rapid internalization, we asked whether $\alpha L/\beta_2$ endocytosis is dependent on the integrity of DRM, thereby indicating that partitioning into lipid rafts would be required for efficient internalization (and recycling) of the adhesion receptor. To address this hypothesis, we performed internalization assays in the presence of the cholesterol-sequestering agents β-methylcyclodextrin (βMCD) and filipin. As shown in Figure 2, pretreatment with 5 μg/ml filipin inhibited fMLF-induced $\alpha L/\beta_2$ internalization in primary neutrophils (Figure 2A, closed triangles), suggesting that fMLF-driven endocytosis and DRM partitioning of $\alpha L/\beta_2$ are functionally linked processes. Treatment with βMCD yielded similar results (our unpublished data). To address whether partitioning of $\alpha L/\beta_2$ into DRM persists after endocytosis, we assessed the relative ratios of the internalized pool of $\alpha L/\beta_2$ in the floating versus nonfloating fractions of a sucrose gradient. To this aim, primary neutrophils were surface labeled with GSH-cleavable biotin at 0°C, followed by fMLF stimulation and reduction of surface-bound biotin with the nonmembrane-permeable agent GSH. The biotinylated (endocytosed) pool of $\alpha L/\beta_2$ was then immunoprecipitated from floating versus nonfloating fractions after Triton X-100 extraction and sucrose gradient centrifugation (Figure 3, top). Normalization was carried out by probing the filters with an anti-αL antibody, to assess the total amount of immunoprecipitated LFA-1 in each lane (Figure 3, bottom). Interestingly, under these conditions >90% of the internalized receptor seems to be DRM associated (Figure 3, top right, compare floating vs. bottom fractions), thus indicating that chemokine-induced partitioning of the adhesion receptor into DRM is persistent and mainly involves an endocytic compartment.

Cholesterol Depletion Inhibits fMLF-induced Cell Migration

We have previously demonstrated that a point mutation (Y735A) in the cytoplasmic domain of β_2 impaired the receptor's endo-exocytic cycle and routed the integrin toward a degradative pathway (Fabbri *et al*., 1999b; Tohyama *et al*., 2003). The $\alpha L/\beta_2^{Y735A}$ mutant receptor efficiently supports ligand recognition and spreading, but it is unable to support

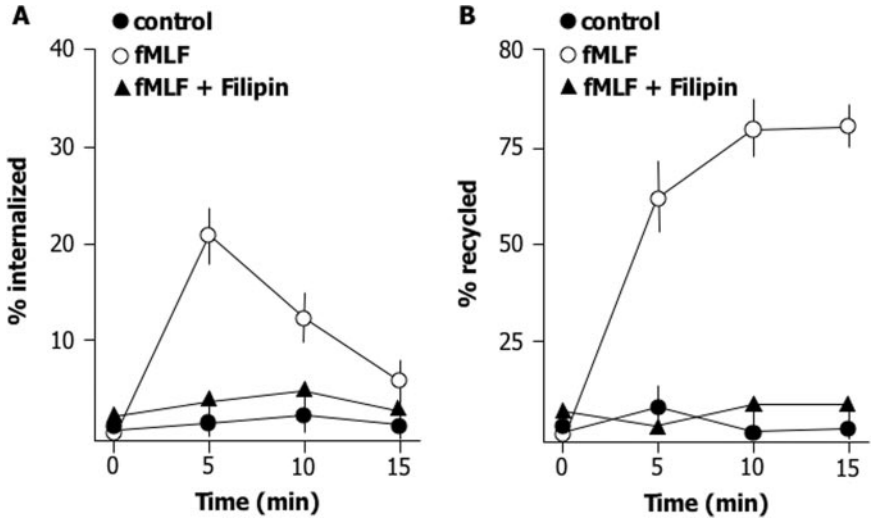

Figure 2. $\alpha L/\beta_2$ internalization is sensitive to cholesterol depletion in chemokine-stimulated PMN. Freshly purified PMN were preincubated in the absence (circles) or presence (closed triangles) of 5 μg/ml filipin, surface labeled with cleavable biotin, and incubated at 37°C for the indicated time points in absence (closed circles) or presence of 100 nM fMLF (open circles). Endocytosis (A) and recycling (B) were assessed as described in *Materials and Methods*. Data are expressed as the percentage of internalization over the total amount of labeled receptor (A) or as the percentage of recycling over the amount of internalized receptor (B). Values represent a mean ± SD of four separate experiments.

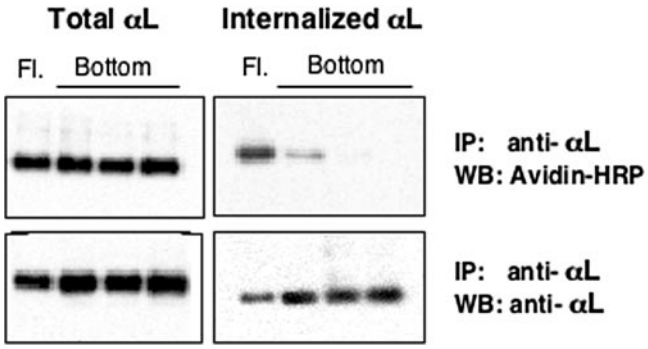

Figure 3. The endocytosed fraction of $\alpha L/\beta_2$ partitions into DRM in PMN. Freshly purified PMN were labeled at 4°C with cleavable biotin and stimulated with 100 nM fMLF for 5 min at 37°C before surface biotin cleavage, lysis, and floatation over a discontinuous step sucrose gradient, as described in *Materials and Methods*. αL was immunoprecipitated either from the pooled floating fractions 9–11 or from the individual bottom fractions 1–3 (see Figure 1). The immunoprecipitated, biotinylated receptor was revealed with avidin-HRP to assess DRM partitioning of the internalized versus total $\alpha L/\beta_2$ (top). The total amount of $\alpha L/\beta_2$ in each lane was determined by immunoblotting with anti-αL antibody.

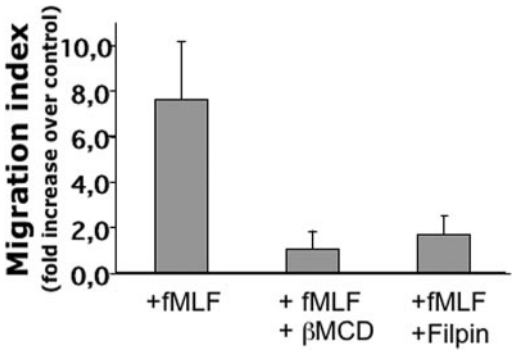

Figure 4. Cholesterol depletion inhibits fMLF-induced PMN migration. Freshly purified PMN were pretreated for 45′ at 37°C in the absence or presence of either 10 mM βMCD or 10 μg/ml filipin, plated on ICAM 1-coated glass-bottom dishes, and analyzed by time-lapse microscopy for 20 min. Then, 100 nM fMLF was added after 5 min. Spontaneous and fMLF-induced cell migration was quantified with Cell Tracker software, as described in *Materials and Methods*. From 30–100 cells for experiment were scored, and the average distance (in micrometers) covered during the observation period was assessed. Data represent the mean ± SD of four separate experiments.

migration on ICAM-1, thereby suggesting that internalization and recycling of the adhesion receptor are important components of directional cell migration (Fabbri *et al*., 1999b; Tohyama *et al*., 2003). To investigate this hypothesis with endogenous $\alpha L/\beta_2$, we performed a quantitative time-lapse analysis of fMLF-induced cell migration, by using PMN pretreated or not with cholesterol-perturbing agents to inhibit fMLF-induced $\alpha L/\beta_2$ internalization.

Freshly purified PMN were pretreated for 45′ at 37°C in the absence or presence of either 10 mM βMCD or 5 μg/ml filipin, plated on ICAM-1-coated glass-bottom dishes, and analyzed by time-lapse videomicroscopy for 20 min, with the addition of 100 nM fMLF after 5 min. As shown in Figure 4, PMN greatly increase their chemokinetic activity after the addition of fMLF. In contrast, cells treated with either βMCD or filipin are unable to migrate (Figure 4 and Supplemental Material S1–S4), despite the fact that their adhesive behavior and fMLF-induced ruffling are not affected by cholesterol sequestration (our unpublished data; Supplemental Material S3).

Endosomal Localization of Internalized $\alpha L/\beta_2$ in PMN

Next, we investigated the endosomal pathway followed by the $\alpha L/\beta_2$ integrin in fMLF-stimulated neutrophils. To avoid artifacts due to receptor clustering, we induced internalization of the adhesion receptor after labeling the surface-expressed pool with a Fab′ fragment of an anti-αL antibody. After endocytosis, cells were processed for immunoelectron microscopy on ultrathin cryosections, and colocalization experiments were carried out using markers of DRM (GM1) and early endosomes (EEA-1). Colocalization of the internalized $\alpha L/\beta_2$ with markers of the recycling compartment (Rab11) was instead assessed by scanning confocal microscopy. Figure 5 shows that as early as 5 min upon fMLF stimulation $\alpha L/\beta_2$ becomes enriched in uncoated membrane invaginations that also contain GM1, whereas the receptor was never observed in clathrin-coated pits or vesicles (our unpublished data). A similar enrichment can be found in an endosomal compartment that also displays a marker of early endosomes (EEA-1). At later time points (20 min), the surface-expressed receptor seems polarized, whereas a large fraction of the endocytosed receptor is found in a $Rab11^+$ recycling compartment (Figure 6), also due to the antibody treatment, which we found to markedly delay receptor recycling (our unpublished data). In contrast, we rarely observed colocalization of endocytosed integrins with LAMP-1, a marker of the late endosomal/lysosomal compartment (Figure 6). Colocalization coefficients were measured using the algorithm provided by the Image-Pro Plus software (Media Cybernetics, Silver Spring, MD). By analyzing at least 20 cells per experiment, we found 43 ± 3% versus 12 ± 4% of endocytosed LFA-1 to be colocalized with $Rab11^+$ or $LAMP\text{-}1^+$ vesicular compartments, respectively. Similar results were obtained by assessing the endocytosis of endogenous β_2 integrins in chemokine-stimulated rat basophilic leukemia (RBL) cells (Supplemental Material S7). These results suggest that independently of receptor clustering, $\alpha L/\beta_2$ follows a clathrin-independent pathway to reach an intracellular recycling compartment.

Internalized αL/β2 Is Sorted to Recycling Endosomes

The findings described above are consistent with the hypothesis that DRM partitioning and endocytosis of $\alpha L/\beta_2$ are interdependent processes and that both are required to support directional motility. To be able to dissect and to genetically manipulate the intracellular sorting pathway followed by the endocytosed integrin, we reconstituted the expression of the fMLF and $\alpha L/\beta_2$ receptors in CHO cells, because the endo-exocytic cycle of LFA-1 as well as of other integrins have been thoroughly characterized in these cells in previous studies (Ylanne *et al*., 1995; Fabbri *et al*., 1999b). fMLF receptor-transfected CHO (HAfpR-CHO) cells displayed a typical chemotactic response to fMLF in transwell assays, which peaked at 1 μM fMLF (due to a reduced ligand affinity of the HA-tagged receptor; our unpublished data). We first determined whether, by analogy with the endogenous receptor in PMN, partitioning of LFA-1 into DRM is an inducible event in HAfpR-CHO transfectants. In these cells, a higher fraction of LFA-1 (8–15%) partitions into DRM under steady-state conditions (our unpublished data).

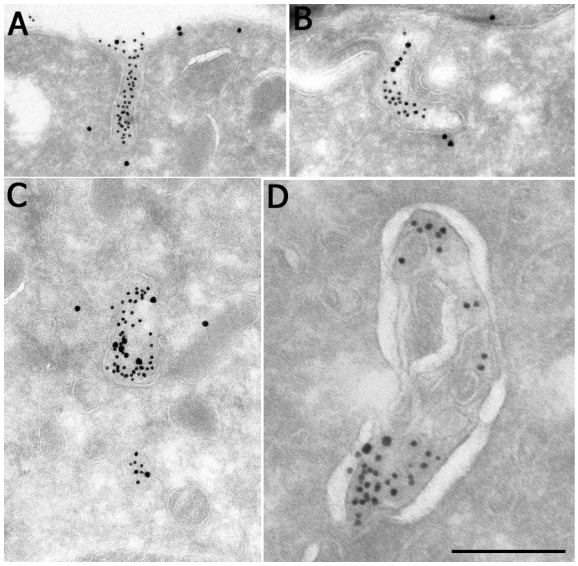

Figure 5. EM analysis of fMLF-induced endosomal localization of $\alpha L/\beta_2$ in PMN. (A–D) Primary PMN were labeled at 4°C with anti-αL Fab′ fragment, incubated at 4°C (A and B) or 37°C (C and D) for 5 min, fixed, and processed for cryo-EM. Panels show ultrathin cryosections double labeled for $\alpha L/\beta_2$ (10-nm gold) and either cholera toxin (15-nm gold; A–C) or EEA-1 (15-nm gold; D). Bar, 0.33 μm (A–C); 0.17 μm (D).

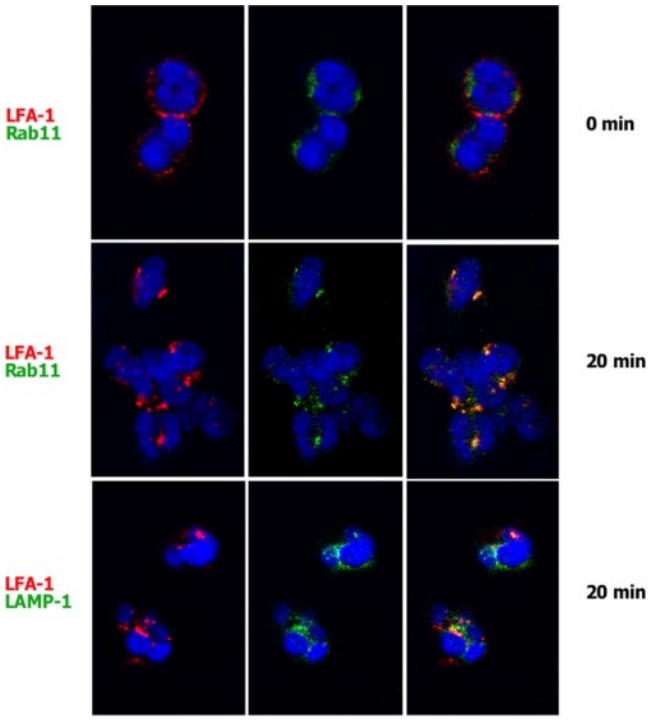

Figure 6. Confocal microscopy analysis of fMLF-induced endosomal localization of $\alpha L/\beta_2$ in PMN. Primary PMN were labeled at 4°C with a Fab′ fragment of an anti-αL mAb, followed by fMLF stimulation and incubation for the indicated time points. Cells were then fixed, permeabilized, and stained with a Cy3-conjugated goat anti-mouse immunoglobulin antiserum (left). Endogenous Rab11 was detected with an affinity-purified rabbit antiserum followed by an FITC-conjugated goat anti-rabbit antibody (top and middle center panels). Endogenous LAMP-1 was detected with an anti-LAMP-1 mAb (IgG_{2b}) followed by a FITC-conjugated, isotype-specific antiserum (bottom center). Nuclei were detected with Hoechst 33342 (blue fluorescence). Right, merged images.

A further increase in the amount of DRM-associated LFA-1 (up to 22%) can be induced by 1 μM fMLF stimulation (our unpublished data). To assess the steady-state subcellular localization of LFA-1 in fMLF-stimulated CHO transfectants, we performed immunogold labeling and electron microscopy analysis on ultrathin cryosections, by using antibodies to αL. Results show that surface-expressed $\alpha L/\beta_2$ is frequently localized within flask-shaped plasma membrane invaginations, morphologically identifiable as caveolae (Supplemental Material S5). To confirm this result, we performed a double immunogold labeling by using anti-αL and anti-caveolin-1 (cav-1) antibodies. As expected, both $\alpha L/\beta_2$ (15 nm), and cav-1 (10 nm) colocalized within the observed flask-shaped invaginations of the plasma membrane or in grape-shaped clusters of caveolae connected to the cell surface (Supplemental Material S6). By morphometric analysis, we evaluated that 51.2% of the total gold particles located on the plasma membrane were associated with either one of these caveolin-1-positive structures, whereas colocalization of $\alpha L/\beta_2$ with clathrin-coated pits was never observed (Supplemental Material S5 and S6). These findings support the assumption that fMLF-induced partitioning of LFA-1 into lipid-ordered membrane domains is not an artifact due to Triton X-100 extraction at 4°C. We next evaluated the distribution of $\alpha L/\beta_2$ within endosomal compartments by immunoelectron microscopy. Results indicate that endosome-associated $\alpha L/\beta_2$ consistently colocalizes with caveolin-1-positive endosomes and with recycling endosomes, as identified by labeling with TfR (Supplemental Material S6). At variance, localization of $\alpha L/\beta_2$ in late endosomes, as identified by M6Pr labeling, was an uncommon event (our unpublished data). Together, these results suggest that both in PMN and in CHO cells $\alpha L/\beta_2$ is preferentially sorted via DRM-enriched membrane subdomains to perinuclear recycling endosomes.

αL/β2 Is Internalized via a Clathrin-independent Pathway in HAfpR-CHO Cells

To functionally dissect the endocytic pathway followed by $\alpha L/\beta_2$, we cotransfected HAfpR-CHO cells with $\alpha L/\beta_2$ and either wild-type or dominant negative mutants of regulatory proteins involved in defined steps of the endocytic process, followed by the quantitative assessment of $\alpha L/\beta_2$ internalization. As a control, we used the TfR, whose clathrin-dependent endocytosis has been extensively documented in most cell types, including CHO cells. Figure 7 shows that, as expected, ligand-induced internalization of TfR is inhibited by DN mutants of Rab5 (N133I), Dynamin (K44A), and Eps15 (Δ95-295). In contrast, the spontaneous internalization of $\alpha L/\beta_2$ was unaffected by the Rab5 and Eps15 DN mutants, whereas it was strongly inhibited by the Dynamin mutant, providing unequivocal evidence that the internalization of $\alpha L/\beta_2$ is at least partially divergent from the classical clathrin-mediated endocytic process.

To address the recycling pathway followed by endocytosed $\alpha L/\beta_2$, we cotransfected HAfpR-CHO cells with GFP-tagged $\alpha L/\beta_2$ and mDSred-tagged constructs coding for either a wild-type or a dominant negative $rab11^{S25N}$ mutant (Wilcke *et al*., 2000) that has been shown to promote the accumulation of recycling receptors in the perinuclear recycling compartment. wt rab11 in CHO cells displays a punctuate staining pattern throughout the cytoplasm, whereas, as

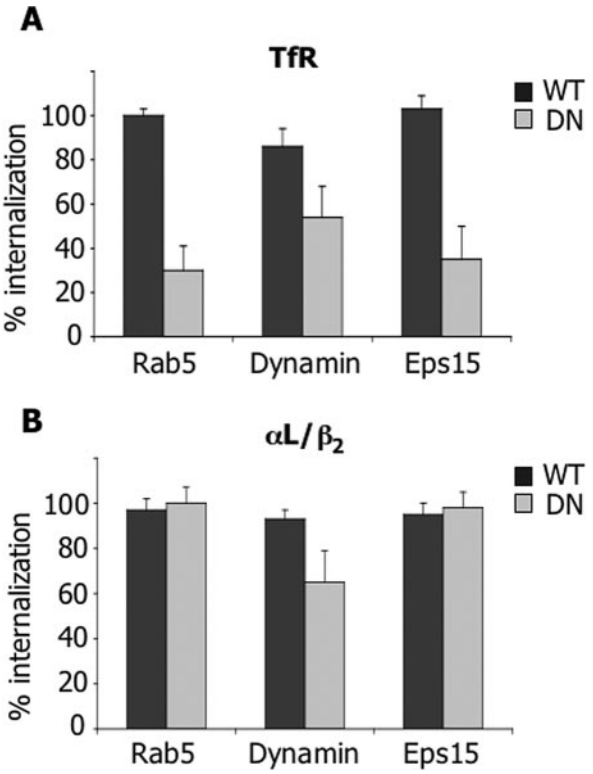

Figure 7. $\alpha L/\beta_2$ internalization does not follow a clathrin-mediated pathway in CHO cells. HAfpR-CHO cells were transiently transfected with either $\alpha L/\beta_2$ (A) or the TfR (B), and cotransfected with either mock cDNA or the indicated wild-type and dominant negative (DN) constructs. Twenty-four hours posttransfection, cells were surface labeled with cleavable biotin at 4°C and stimulated with fMLF (1 μM for 5 min), followed by processing as described in Figure 2 legend. Data are expressed as percentage of internalization over mock-transfected cells. Values represent a mean ± SD of three separate experiments.

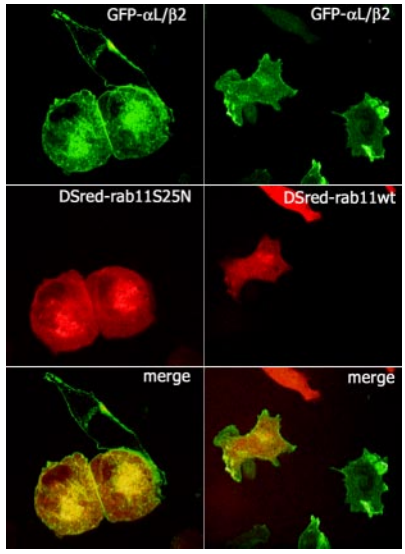

Figure 8. $\alpha L/\beta_2$ is recycled via a Rab11-positive compartment. CHO cells stably expressing the fMLF receptor were transiently transfected with $\alpha L/\beta_2$-GFP and either a wt or a Rab11^{S25N} mutant, expressed as monomeric DsRed chimeric constructs. Twenty-four hours posttransfection, cells were fixed and inspected by laser scanning confocal microscopy.

described previously (Wilcke *et al*., 2000), transient transfection of rab11^{S25N} causes an enlargement of a perinuclear, rab11-positive tubulovesicular compartment (Figure 8) and a rounded cell morphology. As shown in Figure 8, αL-GFP/β_2 accumulates in this rab11-positive compartment, thereby suggesting that the endocytosed receptor transits through a rab11 perinuclear compartment, possibly involved in receptor recycling. The turnover of $\alpha L/\beta_2$ in rab11^{S25N}-expressing cells was quantitatively assessed by flow cytometry, which confirmed an average 30% reduction in the amount of receptor being recycled to the plasma membrane (Supplemental Material S7A). Notably, we observed that cells coexpressing αL-GFP/β_2 and rab11^{S25N} failed to show the characteristic enrichment of this integrin in membrane ruffles (our unpublished data). To rule out that such enrichment was the result of a convoluted arrangement of the plasma membrane at ruffling extensions, we induced ruffling by fMLF stimulation of HAfpR-CHO, transiently cotransfected with αL-GFP/β_2 and either wt rab11 or rab11^{S25N}, followed by ratiometric analysis of αL-GFP/β_2 localization in ruffling versus nonruffling areas of the plasma membrane. Table 1 shows that in wt rab11-transfected cells, αL-GFP/β_2 becomes enriched in ruffling extensions (see Supplemental Material S8). Such enrichment is selectively decreased in rab11^{S25N}-cotransfected cells (Table 1). This finding supports the hypothesis that in chemokine-stimulated cells recycling of $\alpha L/\beta_2$ occurs in a polarized manner toward newly formed membrane extensions.

A Recycling-defective αL/β2 Mutant Dissociates Rapidly from DRM upon fMLF-induced Endocytosis

To better define whether the intracellular sorting of $\alpha L/\beta_2$ is dependent on the nature of the carrier vesicles or on targeting sequences within the integrin's cytoplasmic region, we used HAfpR-CHO cells transiently transfected with the $\alpha L/\beta_2{}^{Y735A}$ mutant integrin ($\alpha L/\beta_2{}^{Y735A}$-CHO), which carries a nonconserved substitution in the membrane proximal Y^{735}RRF endocytic motif. We had previously demonstrated that the $\beta_2{}^{Y735A}$ mutant is internalized with variable kinetics depending on the cell type, but, at variance with the wild-type receptor, it is missorted to a degradative pathway instead of being recycled (Fabbri *et al*., 1999b; Tohyama *et al*., 2003). To investigate the sorting defect in this mutant, we

Table 1. Ratiometric analysis of $\alpha L/\beta_2$ enrichment in ruffles

	αL-GFP/β_2	WGA-TRITC
αL-GFP/β_2 + Rab11 wt[a]	11.7 ± 4.8[b]	1.8 ± 0.3
αL-GFP/β_2 + Rab11^{S25N}	6.4 ± 3.2	1.9 ± 0.7

[a] HAfpR-CHO cells were transiently cotransfected with αL-GFP/β_2 and either Rab11 wt or Rab11^{S25N} constructs. Twenty-four hours posttransfection, cells were stimulated with fMLF to induce ruffling, fixed, and stained with WGA-TRITC to label the plasma membrane (see Supplemental Material S8). Samples were analyzed by scanning confocal microscopy.

[b] Numbers represent the ratio of mean fluorescence values detected in equivalent surface areas drawn around ruffles vs. the ventral aspect of the plasma membrane. At least three selected areas per cell within a sample of 20 cells per experiment were analyzed. Data represent the mean ± SD of three separate experiments.

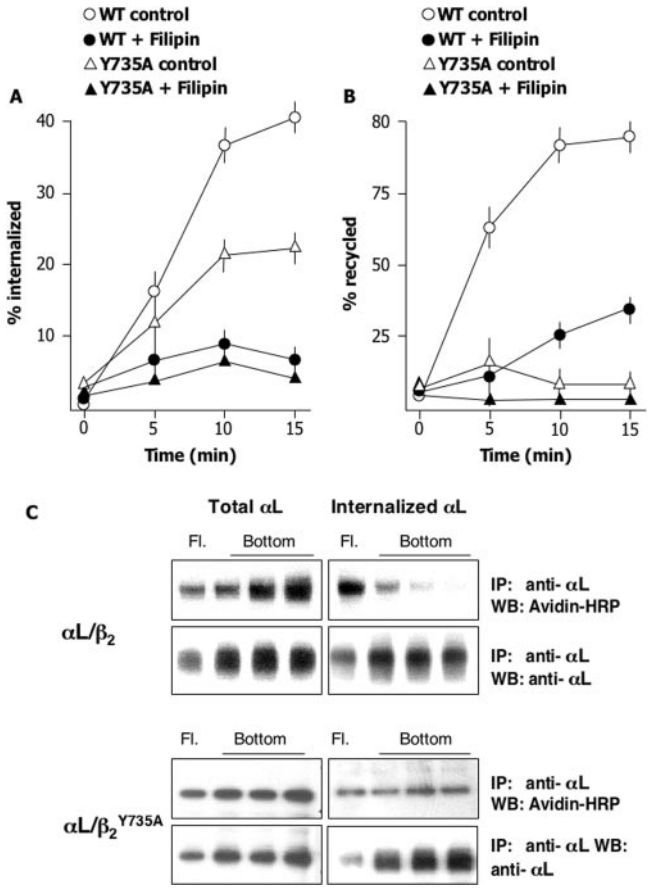

Figure 9. $\alpha L/\beta_2$ wt and $\alpha L/\beta_2^{Y735A}$ mutant internalization involve DRM inclusion and are sensitive to cholesterol depletion in CHO cells. (A) HAfpR-CHO cells were transiently transfected with either $\alpha L/\beta_2$ wt or $\alpha L/\beta_2^{Y735A}$ and preincubated in the absence or presence of 5 μM filipin. Cells were then surface labeled with cleavable biotin at 4°C and processed as described in Figure 2 legend. Data are expressed as the percentage of internalization over the total amount of labeled receptor (A) or as the percentage of recycling over the amount of internalized receptor (B). Values represent a mean ± SD of three separate experiments. (C) HAfpR-CHO cells were transiently transfected with either $\alpha L/\beta_2$ wt or $\alpha L/\beta_2^{Y735A}$, labeled at 4°C with cleavable biotin, and stimulated with 1 μM fMLF for 5 min at 37°C before surface biotin cleavage, lysis, and floatation over a discontinuous step sucrose gradient, as described in *Materials and Methods*. αL was immunoprecipitated either from the pooled floating fractions 9–11 or from the individual bottom fractions 1–3 (see Figure 1). The immunoprecipitated, biotinylated receptor was revealed with avidin-HRP to assess DRM partitioning of the internalized versus total $\alpha L/\beta_2$ (top). The total amount of $\alpha L/\beta_2$ in each lane was determined by immunoblotting with anti-αL antibody.

initially addressed whether the mutant receptor requires integrity of DRM for endocytosis upon chemokine stimulation. Figure 9A shows that after fMLF treatment $\alpha L/\beta_2^{Y735A}$ is internalized with reduced efficiency compared with the wild-type receptor (Figure 9A, compare open circle with open triangles). However, endocytosis of the mutant receptor is sensitive to cholesterol sequestration by filipin, suggesting that DRM partitioning is required (Figure 9A). As shown previously (Fabbri *et al*., 1999a), wild-type $\alpha L/\beta_2$ is efficiently recycled to the plasma membrane, albeit with slower kinetics compared with the endogenous receptor, whereas the $\alpha L/\beta_2^{Y735A}$ mutant is recycled to a negligible extent (Figure 9B). Due to the nature of the assay, receptor recycling was below measurable rates whenever endocytosis was minimal or absent (Figure 9B). To further address this issue, we performed floatation assays on Triton X-100 lysates. Figure 9C shows that a fraction of the $\alpha L/\beta_2^{Y735A}$ mutant, similar to the wild-type receptor, does partition into DRM after chemokine stimulation (Figure 9C, top left). Although most (>80%) of the internalized, wild-type receptor is associated with DRM, indicating that partitioning of LFA-1 into lipid-ordered membrane microdomains persists after endocytosis, the mutant receptor seems to dissociate rapidly from raft-enriched membranes, because only 25% of the internalized receptor can be recovered from the floating fractions of fMLF-stimulated transfectants (Figure 9C, top right). The intracellular sorting pathway of the mutant receptor also was investigated by coimmunolocalization and cryoelectron microscopy. As described above, cells were allowed to internalize 5-nm gold-labeled bovine serum albumin for 1 h to identify endosomal compartments, and then they were processed for cryoimmuno-electron microscopy (EM). Morphometric analysis of replicate experiments showed that only 32% of the $\alpha L/\beta_2^{Y735A}$ mutant colocalized with TfR, whereas ~50% colocalized with M6PR (Supplemental Material S9). These results suggest that endocytosed $\alpha L/\beta_2$ can follow different sorting pathways, depending on defined targeting sequences in the cytoplasmic domain that affect the persistence of DRM association.

DISCUSSION

In this work, we have investigated in detail the endo-exocytic cycle of the leukocyte integrin $\alpha L/\beta_2$, based on the hypothesis that in chemokine-stimulated cells membrane integrin turnover is required to support directionality in leukocyte migration. Our findings show that partitioning of $\alpha L/\beta_2$ into DRM is an inducible process in primary neutrophils and is required for the rapid and efficient internalization of the ligand unengaged receptor. DRM association persists throughout the endo-exocytic cycle of the wild-type receptor, but not of a recycling-defective mutant receptor, supporting the hypothesis that the lipid environment of $\alpha L/\beta_2$-containing endosomal membranes contributes to directing the intracellular routing of the endocytosed receptor.

Previous studies have suggested that the endocytic cycle of integrins is relevant for their physiological role in supporting and maintaining polarity in vectorially migrating cells. By analyzing PMN migrating over a fibronectin matrix, Pierini *et al*. (2000) showed that the α_5/β_1 integrin is present in endocytic vesicles, where it colocalizes with a marker of an endocytic recycling compartment (ERC). In this model, intracellular calcium concentration buffering inhibits cell detachment from the rear edge and results in depletion of α_5/β_1, both from endocytic vesicles and the recycling compartment, suggesting that integrins are normally turned over by endocytosis and recycling during cell migration. This model was further refined by the demonstration that the ERC itself reorients to retain its localization just behind the leading lamella as PMN migrate, indicating that membrane recycling during neutrophil migration has directionality (Pierini *et al*., 2000). Using NIH-3T3 cells migrating over vitronectin, Roberts *et al*. (2001) have shown that the mitogenic effect of platelet-derived growth factor involves recycling of endocytosed α_V/β_3 integrins through Rab4- and Rab11-positive compartments and that dominant interfering Rab4 mutants, by preventing membrane recycling of integrins, abrogate substrate-specific migration. More recently, substrate-dependent internalization and recycling of α_6/β_1 integrin has been shown to be required for rapid neural crest

cell migration (Strachan and Condic, 2003). In previous studies, we have shown that subtle mutations in the β_2-integrin cytoplasmic domain that impair its membrane recycling result in defective migration over the specific ligand ICAM-1 (Fabbri *et al*., 1999b; Tohyama *et al*., 2003). The aforementioned studies emphasize the importance of the endocytic cycle of integrins in supporting vectorial migration, and they suggest that integrin endo-exocytosis must be efficiently controlled for the cell to dynamically redistribute adhesion receptors from the trailing edge to the leading lamellipodium. We asked whether endocytosis of integrins is a regulated event occurring in defined membrane subcompartments. Several independent findings in this work indicate that integrins are endocytosed using a highly efficient, clathrin-independent pathway that involves cholesterol-enriched DRM. First, a sizable fraction of the endogenous receptor can be isolated biochemically in the floating, Triton X-100-insoluble fractions of discontinuous sucrose gradients in chemokine-stimulated PMN. On a quantitative basis, the fraction of $\alpha L/\beta_2$ mobilized into DRM after fMLF stimulation parallels closely the amount of endocytosed receptor under the same conditions. Second, both in neutrophils and in CHO transfectants, membrane-expressed $\alpha L/\beta_2$ localizes preferentially in membrane invaginations resembling caveolae, which are known to be sites of active endocytosis (Kurzchalia and Parton, 1999; Pelkmans and Helenius, 2002). Although in CHO cells the above-mentioned invaginations are enriched in caveolin, in primary neutrophils, which are devoid of caveolin, they contain markers of DRM. Third, the internalization of $\alpha L/\beta_2$ is unaffected by dominant negative mutants of defined components of clathrin-mediated endocytosis, including $Rab5^{N133I}$ and $Eps15^{\Delta 95-295}$, which efficiently prevent the endocytosis of the TfR. Notably, the inhibitory effect of $dynamin^{K44A}$, coupled to clathrin independence, suggests that the endocytic pathway followed by $\alpha L/\beta_2$ resembles that observed for other membrane receptors, such as the interleukin-2 receptor and the common γ chain (Kirkham and Parton, 2005). Finally, functional evidence for the involvement of DRM in $\alpha L/\beta_2$ endocytosis is provided by its selective impairment in cells exposed to cholesterol-sequestering agents, such as filipin or βMCD. An increasing number of membrane-associated proteins has been recently reported to be endocytosed and sorted via DRM and caveolae (Fivaz *et al*., 2002; Sabharanjak *et al*., 2002; Kirkham and Parton, 2005). The existing evidence, however, suggests that the mechanisms underlying this novel endocytic pathway are highly variable, depending on the protein and the cell type under study. For example, routing of endocytosed receptors to recycling endosomes may be particularly efficient in CHO cells, which have been recently reported to preferentially direct internalized GPI-anchored proteins to such compartment (Fivaz *et al*., 2002). Because some of these studies make use of antibodies both to induce and to monitor receptor internalization and recycling, the interpretation of the results may be affected by antibody-induced clustering and by the visualization of the internalized antibody rather than the receptor. In this respect, it is noteworthy that in our model partitioning of the receptor in DRM and its subsequent endocytosis require an activating stimulus but occur in the absence of ligand-induced clustering. This is at variance with the requirement for ligand engagement observed for most receptors internalized via DRM (Simons and Toomre, 2000; Fullekrug and Simons, 2004) and suggests that, in the case of $\alpha L/\beta_2$, inducible connections with either DRM-resident proteins or with cytoskeletal proteins are involved in the rapid partitioning and endocytosis of the receptor. The functional significance of the peculiar endocytic cycle followed by $\alpha L/\beta_2$ remains to be established. Several groups have reported that functional activation of $\alpha L/\beta_2$ leads to its enrichment in rafts, which may be relevant for its adhesive and signaling role (Krauss and Altevogt, 1999; Leitinger and Hogg, 2002). We propose that inclusion into lipid-ordered subdomains of the plasma membrane is required for rapid and efficient endocytosis of the ligand-unengaged receptor. Our demonstration that DRM association persists after endocytosis and is a feature of recycling-competent receptors support the hypothesis that not only endocytosis but also recycling of $\alpha L/\beta_2$ requires partitioning into DRM. In this respect, polarized recycling of $\alpha L/\beta_2$-containing vesicles to the leading edge of migrating cells could promote the progressive enrichment of raft-resident proteins and lipids at the front of the cell, thus contributing to the creation of a structural and functional asymmetry of the plasma membrane of directionally migrating cells. Such asymmetric distribution of membrane components has been thoroughly characterized in several models (Gomez-Mouton *et al*., 2001; Millan *et al*., 2002; Manes *et al*., 2003; Pierini *et al*., 2003), but questions remain concerning the mechanisms underlying its onset and maintenance. In apparent contrast with our hypothesis, several studies have shown that fluorescent lipid analogs intercalating into lipid-ordered domains are preferentially sorted into a late endosomal/lysosomal pathway, whereas lipid probes for nonraft membranes enter a recycling pathway (Mukherjee and Maxfield, 2000; van der Goot and Gruenberg, 2002; Hao *et al*., 2004). Notwithstanding the potential distortion of the lipid bilayer generated by the use of intercalating fluorescent lipid probes in living cells (van Meer and Sprong, 2004), such contrasting evidence can be reconciled with our findings by postulating the existence of heterogeneous lipid-ordered microdomains, characterized by qualitatively and quantitatively different protein cargoes and following variable intracellular routes. Evidence in favor of this interpretation is indeed accumulating, particularly in model systems not requiring receptor clustering for the microscopic visualization of rafts. Using such models, rafts can be visualized as small dynamic assemblies wherein resident proteins are preferentially associated with certain types of lipids. These "shells" are thermodynamically stable, mobile entities in the plane of the membrane that are able to target the protein they encase to preexisting rafts/caveolae domains, either on the plasma membrane or in endosomal compartments, thus adding complexity to the issue of what structural determinants dictate intracellular protein sorting (Zacharias *et al*., 2002; Helms and Zurzolo, 2004; Mayor and Riezman, 2004).

In conclusion, our work indicates that leukocyte integrins can be endocytosed through a pathway involving DRM, thus delineating an alternative route for internalizing rapidly and efficiently ligand-unengaged integral membrane proteins and directing them to an early endosomal compartment. Whether localization in DRM affects the subsequent fate of the endocytosed receptors remains to be unequivocally established. Partitioning into DRM of endocytosed integrins may be involved in directing them to a recycling compartment, and later on, to sorting vesicles emerging in a polarized manner toward the DRM-enriched leading edge of migrating cells. We propose a model whereby the observed endo-exocytic cycle of integrins is functional to retrieve these receptors with high efficiency, as they detach from their ligands, and to reuse them in areas of the plasma membrane where they have to establish new adhesive interactions. Our hypothesis is consistent with the observation that polarized leukocytes display both leading- and trailing-edge rafts (Gomez-Mouton *et al*., 2001) and with the recent

demonstration that in migrating cells endocytically active membrane domains localize at the cell rear (Beardsley *et al*., 2005). Ligand-unengaged integrins could be preferentially internalized at the trailing edge and recycled, along with raft components, to the leading edge of directionally migrating cells, thus contributing to the maintenance of rear–front polarity.

ACKNOWLEDGMENTS

We thank Stella Putignano for technical help, Chanel Smart for critical discussion, and Andrea Giacosi and Alessandra Sirri for developing the cell tracker software (Cellbuster). Part of this work was carried out in Alembic, an advanced microscopy laboratory established by the San Raffaele Scientific Institute and the Vita-Salute San Raffele University. This work was supported in part by grants from the European Union (MAIN Network of Excellence, FP6-502935) to R. P.; from Associazione e della Fondazione Italiana per la Ricerca sul Cancro and Ministero dell'Istruzione, dell'Università e della Ricerca (MIUR) (PRIN projects) to R. P. and C. T.; from Fondazione Italiana per la Ricerca sul Cancro to C. T.; and from National Institutes of Health Grant R01 HL43331 and the Raymond and Beverly Sackler Foundation to J.R.B. This study was carried out in the framework of the Italian MUIR Center of Excellence in Physiopathology of Cell Differentiation. The electron microscopy work has been performed by the Telethon Facility for Electron Microscopy, Genoa, Italy (Telethon grant GTF03001 to C. T.).

REFERENCES

Beardsley, A., Fang, K., Mertz, H., Castranova, V., Friend, S., and Liu, J. (2005). Loss of caveolin-1 polarity impedes endothelial cell polarization and directional movement. J. Biol. Chem. *280*, 3541–3547.

Bianchi, E., Bender, J. R., Blasi, F., and Pardi, R. (1997). Through and beyond the wall: late steps in leukocyte transendothelial migration. Immunol. Today *18*, 586–591.

Bretscher, M. S., and Aguado-Velasco, C. (1998). Membrane traffic during cell locomotion. Curr. Opin. Cell Biol. *10*, 537–541.

Brown, D. A., and Rose, J. K. (1992). Sorting of GPI-anchored proteins to glycolipid-enriched membrane subdomains during transport to the apical cell surface. Cell *68*, 533–544.

Clark, R. A., and Nauseef, W. M. (1996). Isolation and functional analysis of neutrophils. In: Current Protocols in Immunology, vol. 2, ed. J. E. Coligan, A. M. Kruisbeek, D. H. Margulies, E. M. Shevach, and W. Strober, Edison, NJ: John Wiley & Sons, 7.23.21.

Confalonieri, S., Salcini, A. E., Puri, C., Tacchetti, C., and Di Fiore, P. P. (2000). Tyrosine phosphorylation of Eps15 is required for ligand-regulated, but not constitutive, endocytosis. J. Cell Biol. *150*, 905–912.

Devreotes, P., and Janetopoulos, C. (2003). Eukaryotic chemotaxis: distinctions between directional sensing and polarization. J. Biol. Chem. *278*, 20445–20448.

Eaton, S., and Simons, K. (1995). Apical, basal, and lateral cues for epithelial polarization. Cell *82*, 5–8.

Fabbri, M., Bianchi, E., Fumagalli, L., and Pardi, R. (1999a). Regulation of lymphocyte traffic by adhesion molecules. Inflamm. Res. *48*, 239–246.

Fabbri, M., Fumagalli, L., Bossi, G., Bianchi, E., Bender, J. R., and Pardi, R. (1999b). A tyrosine-based sorting signal in the beta2 integrin cytoplasmic domain mediates its recycling to the plasma membrane and is required for ligand-supported migration. EMBO J. *18*, 4915–4925.

Fivaz, M., Vilbois, F., Thurnheer, S., Pasquali, C., Abrami, L., Bickel, P. E., Parton, R. G., and van der Goot, F. G. (2002). Differential sorting and fate of endocytosed GPI-anchored proteins. EMBO J. *21*, 3989–4000.

Fullekrug, J., and Simons, K. (2004). Lipid rafts and apical membrane traffic. Ann. NY Acad. Sci. *1014*, 164–169.

Funamoto, S., Meili, R., Lee, S., Parry, L., and Firtel, R. A. (2002). Spatial and temporal regulation of 3-phosphoinositides by PI 3-kinase and PTEN mediates chemotaxis. Cell *109*, 611–623.

Gomez-Mouton, C., Abad, J. L., Mira, E., Lacalle, R. A., Gallardo, E., Jimenez-Baranda, S., Illa, I., Bernad, A., Manes, S., and Martinez, A. C. (2001). Segregation of leading-edge and uropod components into specific lipid rafts during T cell polarization. Proc. Natl. Acad. Sci. USA *98*, 9642–9647.

Hao, M., Mukherjee, S., Sun, Y., and Maxfield, F. R. (2004). Effects of cholesterol depletion and increased lipid unsaturation on the properties of endocytic membranes. J. Biol. Chem. *279*, 14171–14178.

Helms, J. B., and Zurzolo, C. (2004). Lipids as targeting signals: lipid rafts and intracellular trafficking. Traffic *5*, 247–254.

Iijima, M., and Devreotes, P. (2002). Tumor suppressor PTEN mediates sensing of chemoattractant gradients. Cell *109*, 599–610.

Kirkham, M., and Parton, R. G. (2005). Clathrin-independent endocytosis: new insights into caveolae and non-caveolar lipid raft carriers. Biochim. Biophys. Acta *1745*, 273–286.

Krauss, K., and Altevogt, P. (1999). Integrin leukocyte function-associated antigen-1-mediated cell binding can be activated by clustering of membrane rafts. J. Biol. Chem. *274*, 36921–36927.

Kurzchalia, T. V., and Parton, R. G. (1999). Membrane microdomains and caveolae. Curr. Opin. Cell Biol. *11*, 424–431.

Lauffenburger, D. A., and Horwitz, A. F. (1996). Cell migration: a physically integrated molecular process. Cell *84*, 359–369.

Lawson, M. A., and Maxfield, F. R. (1995). Ca(2+)- and calcineurin-dependent recycling of an integrin to the front of migrating neutrophils. Nature *377*, 75–79.

Leitinger, B., and Hogg, N. (2002). The involvement of lipid rafts in the regulation of integrin function. J. Cell Sci. *115*, 963–972.

Lokuta, M. A., Nuzzi, P. A., and Huttenlocher, A. (2003). Calpain regulates neutrophil chemotaxis. Proc. Natl. Acad. Sci. USA *100*, 4006–4011.

Manahan, C. L., Iglesias, P. A., Long, Y., and Devreotes, P. N. (2004). Chemoattractant signaling in *Dictyostelium discoideum*. Annu. Rev. Cell Dev. Biol. *20*, 223–253.

Manes, S., Ana Lacalle, R., Gomez-Mouton, C., and Martinez, A. C. (2003). From rafts to crafts: membrane asymmetry in moving cells. Trends Immunol. *24*, 320–326.

Manes, S., Mira, E., Gomez-Mouton, C., Lacalle, R. A., Keller, P., Labrador, J. P., and Martinez, A. C. (1999). Membrane raft microdomains mediate front-rear polarity in migrating cells. EMBO J. *18*, 6211–6220.

Manes, S., Mira, E., Gomez-Mouton, C., Lacalle, R. A., and Martinez, C. (2000). Cells on the move: a dialogue between polarization and motility. IUBMB Life *49*, 89–96.

Mayor, S., and Riezman, H. (2004). Sorting GPI-anchored proteins. Nat. Rev. Mol. Cell. Biol. *5*, 110–120.

McKay, D. A., Kusel, J. R., and Wilkinson, P. C. (1991). Studies of chemotactic factor-induced polarity in human neutrophils. Lipid mobility, receptor distribution and the time-sequence of polarization. J. Cell Sci. *100*, 473–479.

Merlot, S., and Firtel, R. A. (2003). Leading the way: directional sensing through phosphatidylinositol 3-kinase and other signaling pathways. J. Cell Sci. *116*, 3471–3478.

Millan, J., Montoya, M. C., Sancho, D., Sanchez-Madrid, F., and Alonso, M. A. (2002). Lipid rafts mediate biosynthetic transport to the T lymphocyte uropod subdomain and are necessary for uropod integrity and function. Blood *99*, 978–984.

Mukherjee, S., and Maxfield, F. R. (2000). Role of membrane organization and membrane domains in endocytic lipid trafficking. Traffic *1*, 203–211.

Nebl, T., Pestonjamasp, K. N., Leszyk, J. D., Crowley, J. L., Oh, S. W., and Luna, E. J. (2002). Proteomic analysis of a detergent-resistant membrane skeleton from neutrophil plasma membranes. J. Biol. Chem. *277*, 43399–43409.

Pelkmans, L., and Helenius, A. (2002). Endocytosis via caveolae. Traffic *3*, 311–320.

Pierini, L. M., Eddy, R. J., Fuortes, M., Seveau, S., Casulo, C., and Maxfield, F. R. (2003). Membrane lipid organization is critical for human neutrophil polarization. J. Biol. Chem. *278*, 10831–10841.

Pierini, L. M., Lawson, M. A., Eddy, R. J., Hendey, B., and Maxfield, F. R. (2000). Oriented endocytic recycling of $\alpha 5\beta 1$ in motile neutrophils. Blood *95*, 2471–2480.

Ridley, A. J., Schwartz, M. A., Burridge, K., Firtel, R. A., Ginsberg, M. H., Borisy, G., Parsons, J. T., and Horwitz, A. R. (2003). Cell migration: integrating signals from front to back. Science *302*, 1704–1709.

Roberts, M., Barry, S., Woods, A., van der Sluijs, P., and Norman, J. (2001). PDGF-regulated rab4-dependent recycling of alphavbeta3 integrin from early endosomes is necessary for cell adhesion and spreading. Curr. Biol. *11*, 1392–1402.

Sabharanjak, S., Sharma, P., Parton, R. G., and Mayor, S. (2002). GPI-anchored proteins are delivered to recycling endosomes via a distinct cdc42-regulated, clathrin-independent pinocytic pathway. Dev. Cell *2*, 411–423.

Simons, K., and Ikonen, E. (1997). Functional rafts in cell membranes. Nature *387*, 569–572.

Simons, K., and Toomre, D. (2000). Lipid rafts and signal transduction. Nat. Rev. Mol. Cell. Biol. *1*, 31–39.

Slaughter, N., Laux, I., Tu, X., Whitelegge, J., Zhu, X., Effros, R., Bickel, P., and Nel, A. (2003). The flotillins are integral membrane proteins in lipid rafts that contain TCR-associated signaling components: implications for T-cell activation. Clin. Immunol. *108*, 138–151.

Springer, T. A. (1994). Traffic signals for lymphocyte recirculation and leukocyte emigration: the multistep paradigm. Cell *76*, 301–314.

Strachan, L. R., and Condic, M. L. (2003). Neural crest motility and integrin regulation are distinct in cranial and trunk populations. Dev. Biol. *259*, 288–302.

Tohyama, Y., Katagiri, K., Pardi, R., Lu, C., Springer, T. A., and Kinashi, T. (2003). The critical cytoplasmic regions of the alphaL/beta2 integrin in Rap1-induced adhesion and migration. Mol. Biol. Cell *14*, 2570–2582.

van der Goot, F. G., and Gruenberg, J. (2002). Oiling the wheels of the endocytic pathway. Trends Cell Biol. *12*, 296–299.

van Meer, G., and Sprong, H. (2004). Membrane lipids and vesicular traffic. Curr. Opin. Cell Biol. *16*, 373–378.

Varma, R., and Mayor, S. (1998). GPI-anchored proteins are organized in submicron domains at the cell surface. Nature *394*, 798–801.

Wilcke, M., Johannes, L., Galli, T., Mayau, V., Goud, B., and Salamero, J. (2000). Rab11 regulates the compartmentalization of early endosomes required for efficient transport from early endosomes to the trans-Golgi network. J. Cell Biol. *151*, 1207–1220.

Ylanne, J., Huuskonen, J., O'Toole, T. E., Ginsberg, M. H., Virtanen, I., and Gahmberg, C. G. (1995). Mutation of the cytoplasmic domain of the integrin beta 3 subunit. Differential effects on cell spreading, recruitment to adhesion plaques, endocytosis, and phagocytosis. J. Biol. Chem. *270*, 9550–9557.

Zacharias, D. A., Violin, J. D., Newton, A. C., and Tsien, R. Y. (2002). Partitioning of lipid-modified monomeric GFPs into membrane microdomains of live cells. Science *296*, 913–916.

Zurzolo, C., van't Hof, W., van Meer, G., and Rodriguez-Boulan, E. (1994). VIP21/caveolin, glycosphingolipid clusters and the sorting of glycosylphosphatidylinositol-anchored proteins in epithelial cells. EMBO J. *13*, 42–53.